Pergamon

*Deep-Sea Research I*, Vol. 43, No. 7, pp. 1105–1122, 1996

0967–0637/96 $15.00+0.00

PII: S0967–0637(96)00047–7

# Mean annual variation of transport of major currents in the tropical Pacific Ocean

JEAN-RENE DONGUY* and GARY MEYERS†

(*Received* 28 *November* 1994; *in revised form* 31 *July* 1995; *accepted* 19 *February* 1996)

**Abstract**—Expendable bathythermograph (XBT) data and the climatological temperature/salinity relationship were used to calculate the mean annual cycle of dynamic height and geostrophic transport of major currents relative to 400 db along five shipping tracks covering a large part of the tropical Pacific Ocean. The data were selected in bands centered on the most frequently repeated XBT tracklines for the period 1967–1988. Long-term bimonthly mean temperature was calculated in 1° latitude bins along the tracks. The transport function (vertically integrated dynamic height) was then calculated using the mean temperature/salinity relationship. The mean annual cycle of transport of the North Equatorial Current (NEC), the North Equatorial Countercurrent (NECC) and the South Equatorial Current (SEC) (south of 2.5°S) were determined between the ridges and troughs of the transport function. The stochastic errors in bimonthly mean transports were 1–2 Sverdrups on the most sampled tracks. Mean transports of the NEC and NECC increase regularly with longitude from east to west. The NECC has a large annual cycle with a transport-maximum during northern fall and winter. Seasonal variations of the NEC are small. Seasonal variations of the SEC are slightly larger, and they have considerably different phase from track to track. The variation of thermal structure associated with the currents is described. The results of this study are compared in detail to the results of earlier studies of the transports. The differences between the studies are larger than the expected stochastic errors in the mean transports due to differences in the definition of boundaries of the currents and to differences in the procedure for calculating the mean annual variation. The results of all the studies are summarised to facilitate future comparisons to ocean general circulation models and other applications. Copyright © 1996 Elsevier Science Ltd

## INTRODUCTION

Due to its large size, the variation of general circulation of the Pacific Ocean has rarely been described in its totality using hydrographic data, with the exception of the study of dynamic height by Wyrtki (1974a). The number of available hydrographic stations is generally too small for basin-wide studies. There have, however, been a number of regional studies. The western Pacific currents have been described by Merle *et al.* (1969), who noted in the southern hemisphere two shallow countercurrents embedded in a large westward current. Donguy *et al.* (1984) described interannual fluctuations. Delcroix *et al.* (1987) described the currents at 165°E with special attention on the countercurrents. In the central Pacific, the Hawaii–Tahiti Shuttle Experiment provided very detailed information on an annual cycle of the Equatorial Current System (Cantos-Figuerola and Taft, 1983). Wyrtki and Kilonsky (1984) studied mainly westward currents and particularly the South Equatorial Current, whereas Eldin (1983) focused on eastward currents south of the equator. Wyrtki

* CSIRO Division of Oceanography, GPO Box 1538, Hobart, TAS 7001, Australia.
† CSIRO/ORSTOM Centre de Brest, BP 70, 29280 Plouzane, France.

and Kendall (1967) made an early description of the North Equatorial Countercurrent. The eastern Pacific currents have been described by Hayes *et al.* (1983). Wyrtki (1974b) used sea level to document fluctuations of the currents on a large scale throughout the basin.

The development of the expendable bathythermograph (XBT) programme across the Pacific has provided basin-wide observations of the thermal structure of the currents since the 1970s. In this study the widely dispersed sampling is used to document variability of the major, tropical currents throughout the ocean basin.

The thermal data have been used to document the currents on individual sections in several earlier studies (Meyers and Donguy, 1984; Donguy *et al.*, 1986; McPhaden *et al.*, 1988; Harrison *et al.*, 1989). In particular, three studies concentrated on volume transports of the major currents using the XBT data with a climatological temperature/salinity ($T/S$) relationship. Kessler and Taft (1987) (KT) described transports in the central Pacific with emphasis on the 1982–1983 ENSO. Picaut and Tournier (1991) (PT) described interannual variations and developed a method based on the equatorial form of the geostrophic relationship to include currents on the equator. Their data set covered a longer period of time (1979–1985) than KT and included the central and western Pacific. Taft and Kessler (1991) (TK) extended the central Pacific study to cover the period 1970–1987.

The methods used in the three studies are considerably different to ours. In order to maximize the number of available data for studying interannual variations, the three studies selected XBT data from wide bands along the tracks. In some cases the bands had a quite irregular shape to capture as much data as possible. The mean annual variation was not the main issue in these papers, and Taft and Kessler specifically estimated a mean annual cycle for a limited period, 1974–1981, to avoid the effect of El Niño Southern Oscillation on the averaging (Meyers, 1982). The three studies used very careful but subjective methods to define the boundaries of the currents. We felt that there are now enough data to estimate the mean annual variation of major currents in a direct and objective way on narrow well defined tracks.

All the available XBT data were used in this study to describe the mean annual cycle of transports of the North Equatorial Current (NEC), North Equatorial Countercurrent (NECC), and South Equatorial Current south of 2.5°S (SEC) on five of the most frequently repeated and systematically monitored tracks. We chose to use all of the data for as long a period as possible so that the results will be comparable to ocean general circulation models forced with climatological wind stress fields, which are also usually determined from all the available data. The study focused on narrow bands where the XBT data are concentrated, and used a simple and objective procedure to define boundaries of the currents. The result is a succinct description of the annual cycles. The studies described above were restricted to individual tracks in the western and central Pacific, whereas this study used all of the repeated XBT lines throughout the Pacific. The selection and processing of data differs in important ways from the earlier studies, as explained in detail in the discussion.

## DATA AND DATA PROCESSING

Sampling of the tropical Pacific began in 1967 shortly after the XBT was developed. Since the 1970s, routine, systematic coverage has been gradually extended over the following frequently repeated tracks (Fig. 1).

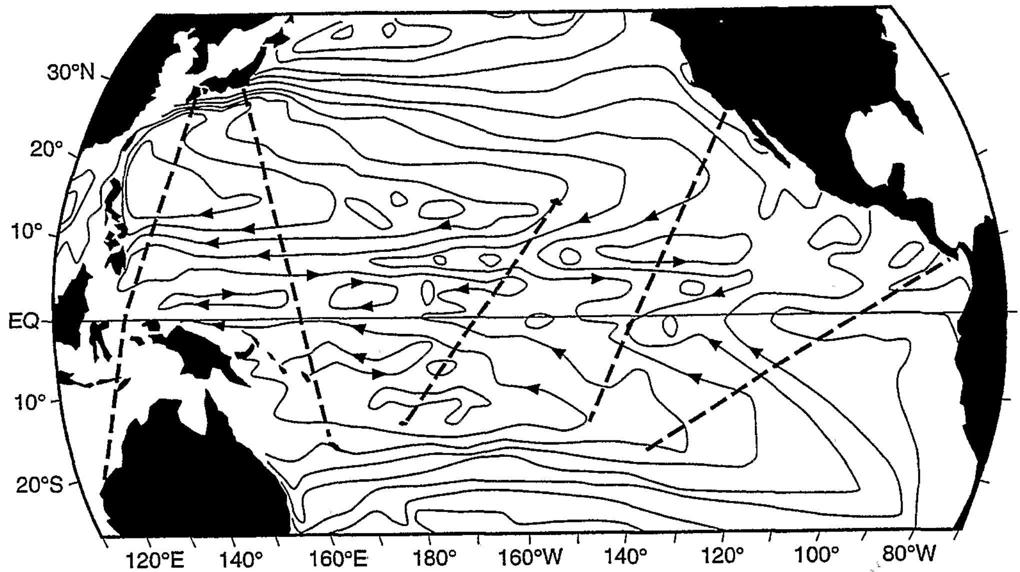


Fig. 1. Tropical Pacific XBT network and mean annual dynamic topography of the sea surface relative to 500 db in dyn cm (from Wyrtki, 1974a).

| | | |
|---|---|---|
| Mururoa–Panama | since 1979 | crossing equator at 110°W |
| Tahiti–Los Angeles | since 1983 | crossing equator at 140°W |
| Auckland–Hawaii | since 1972 | crossing equator at 160°W |
| Nouméa–Japan | since 1979 | crossing equator at 155°E |
| Port Hedland–Japan | since 1985 | crossing equator at 120°E |

See Table 1 for the locations of the ports.

These tracks were selected by the TOGA/WOCE XBT Programme as frequently repeated lines to be covered 18 times per year with 60 miles between XBT drops (Meyers *et al.*, 1991) for the purpose of observing temporal variability of major currents. This mode of sampling is more intensive than the broadscale, low density sampling defined by the Programme for monitoring thermal structure. All the above tracks have been covered at least 12 times per

*Table 1. Location (latitude and longitude) of the ports ending the tracks*

| Port | Latitude | Longitude |
|---|---|---|
| Panama | 8°57N | 79°33W |
| Mururoa | 21°50S | 138°53W |
| Tahiti | 17°33S | 149°37W |
| Los Angeles | 34°00N | 118°15W |
| Auckland | 36°51S | 174°46E |
| Hawaii | 21°18S | 157°52W |
| Nouméa | 22°16S | 166°27E |
| Port Hedland | 20°19S | 118°34E |

year since started, and for extended periods 18 times per year was achieved on some lines. Prior to 1979 the sampling rates were much less frequent. The data base used for this study was assembled by Kessler (1990) after very careful quality control. The XBTs were selected in bands of width 12° longitude centered on the tracklines. The data covered the region 30°N to 30°S and the period 1967–1988. The data set was supplemented with more recent data for the westernmost track. The number of observations on the tracks (Table 2) ranges from 31,845 on the oldest (Auckland–Hawaii) to 1962 on the newest (Port Hedland–Japan).

The XBTs were analysed on the tracks to document the major currents, shown on the map of dynamic height from Wyrtki (1974b) (Fig. 1). The westward NEC is located from about 20°N to 8°N, the eastward NECC from 8°N to 4°N and the SEC south of 4°N extending into the southern hemisphere. The XBTs were binned by 1° latitude along the tracks, and bimonthly averaged temperature at each 20 m depth was calculated. Then dynamic height and the geostrophic transport function (vertically integrated dynamic height) relative to 400 db were calculated using the climatological $T/S$ relationship (Levitus, 1982) interpolated to each bin. The bimonthly averages were calculated for overlapping bimonths (January/February, February/March, etc.), giving 12 values to better delineate the annual cycles.

The boundaries of the currents were identified as the ridges and troughs in the transport function, which are almost identical to the ridges and troughs in the dynamic height field named by Wyrtki (1974a). It is worth noting that sampling on the Auckland–Hawaii track extends northward past Hawaii to the northern boundary of the NEC. The latitudes of the current-boundaries vary during the annual cycle as described in Table 3. The NECC trough is in good agreement with the latitude described for the central Pacific by Taft and Kessler, but the other boundaries do not in all cases match the boundaries used in earlier studies (as discussed in a later section: Comparison to Earlier Studies). The eddies that are common in synoptic, monthly sections across these currents (Wyrtki, 1982) were very weak or nonexistent in the long term bimonthly averages so that identifying the boundaries of the NEC and NECC in the transport functions was perfectly clear.

The major current in the southern hemisphere is the SEC (Fig. 1). The transport of the SEC was estimated as all of the westward vertically-integrated flow south of 2.5°S. The present study does not include the equatorial area (2.5°S–2.5°N), where substantial smoothing of data is required to estimate velocity (Picaut and Tournier). Eastward currents embedded in the SEC appeared in the 0/400 db transports during some bimonths. According to Merle *et al.* (1969) they are the equatorial jets (3°N–3°S), the South Equatorial Countercurrent (SECC) (5°S–10°S) and the South Tropical Countercurrent (STCC) (14°S–18°S). These eastward currents are generally weak and shallow, appearing in the upper 200 m. Their boundaries and strength vary not only annually but also with El Niño Southern Oscillation conditions. They did not have a clear annual cycle in the 0/400 db transports; consequently they are not discussed further in this paper except to mention their long term mean values.

The error in estimating the bimonthly mean transports is largely due to the statistical sampling errors associated with small scale variability that is not well resolved by the XBT sampling, such as eddies and internal waves, or due to variation of the $T/S$ relationship. Both of the errors are discussed below.

In the following discussion of statistical errors the main point is that the standard error of bimonthly means depends mainly on the number of XBT sections available for the study. The statistical error was estimated using a two-layer model of the ocean and propagation of error formulae (Ku, 1966). This approach is necessary because the transports were

*Table 2. Standard error (E) in mean values of the transport*

| Track | Number of XBTs | Number of transects total | NEC $D_N$ (m) | NEC $D_S$ (m) | NEC $C$ (m/s) | NEC Std Dev (Sv) | NEC $E$ (Sv) | NECC $D_N$ (m) | NECC $D_S$ (m) | NECC $C$ (m/s) | NECC Std Dev (Sv) | NECC $E$ (Sv) | SEC $D_N$ (m) | SEC $D_S$ (m) | SEC $C$ (m/s) | SEC Std Dev (Sv) | SEC $E$ (Sv) |
|---|---|---|---|---|---|---|---|---|---|---|---|---|---|---|---|---|---|
| Port Hedland–Japan | 1962 | 49 | 200 | 100 | 1003 | 10.4 | 3.6 | 160* | 215* | 1299 | 16.1 | 5.6 | | | | | |
| Noumea–Japan | 16,118 | 268 | 195 | 135 | 1222 | 13.4 | 2.0 | 135 | 180 | 1481 | 15.5 | 2.3 | 175 | 210 | 1224 | 15.5 | 2.3 |
| Auckland–Hawaii | 31,845 | 530 | 160 | 95 | 923 | 8.0 | 0.8 | 95 | 140 | 1342 | 10.6 | 1.1 | 145 | 230 | 947 | 11.9 | 1.3 |
| Tahiti–Los Angeles | 7417 | 148 | 105 | 50 | 38 | 5.2 | 1.0 | 50 | 125 | 914 | 5.8 | 1.2 | 110 | 230 | 811 | 9.6 | 1.9 |

*Depth of the 20°C isotherm used in all cases except 14°C used here.

*Table 3. Boundaries and mean latitude of the currents*

| | | January | February | March | April | May | June | July | August | September | October | November | December |
|---|---|---|---|---|---|---|---|---|---|---|---|---|---|
| Japan | | 18.5N | 18.5 | 18.5 | 18.5 | 18.5 | 18.5 | 18.5 | 18.5 | 18.5 | 18.5 | 18.5 | 18.5 |
| | NEC | | | | | | | | | | | | |
| | | 7.5 | 7.5 | 7.5 | 7.5 | 7.5 | 7.5 | 7.5 | 7.5 | 7.5 | 7.5 | 7.5 | 7.5 |
| | NECC | | | | | | | | | | | | |
| Port Hedland | | 2.5N | 2.5 | 2.5 | 2.5 | 2.5 | 2.5 | 2.5 | 2.5 | 2.5 | 2.5 | 2.5 | 2.5 |
| Japan | | 18.5N | 19.5 | 16.5 | 17.5 | 17.5 | 17.5 | 19.5 | 19.5 | 19.5 | 18.5 | 18.5 | 18.5 |
| | NEC | | | | | | | | | | | | |
| | | 8.5 | 8.5 | 8.5 | 7.5 | 7.5 | 6.5 | 7.5 | 7.5 | 7.5 | 7.5 | 9.5 | 7.5 |
| | NECC | | | | | | | | | | | | |
| | | 2.5N | 2.5 | 4.5 | 4.5 | 2.5 | 2.5 | 2.5 | 2.5 | 2.5 | 2.5 | 2.5 | 2.5 |
| | | 2.5S | 2.5 | 2.5 | 2.5 | 2.5 | 2.5 | 2.5 | 2.5 | 2.5 | 2.5 | 2.5 | 2.5 |
| | SEC | | | | | | | | | | | | |
| Noumea | | 21.5S | 19.5 | 19.5 | 18.5 | 18.5 | 19.5 | 15.5 | 15.5 | 19.5 | 16.5 | 16.5 | 15.5 |
| Hawaii | | 22.5N | 24.5 | 22.5 | 23.5 | 18.5 | 19.5 | 17.5 | 18.5 | 18.5 | 19.5 | 18.5 | 19.5 |
| | NEC | | | | | | | | | | | | |
| | | 8.5 | 8.5 | 8.5 | 7.5 | 8.5 | 8.5 | 9.5 | 9.5 | 9.5 | 9.5 | 10.5 | 9.5 |
| | NECC | | | | | | | | | | | | |
| | | 2.5N | 4.5 | 4.5 | 2.5 | 2.5 | 2.5 | 4.5 | 4.5 | 4.5 | 4.5 | 4.5 | 4.5 |
| | | 2.5S | 2.5 | 2.5 | 3.5 | 2.5 | 2.5 | 2.5 | 2.5 | 2.5 | 2.5 | 2.5 | 2.5 |
| | SEC | | | | | | | | | | | | |
| Auckland | | 21.5S | 21.5 | 19.5 | 21.5 | 18.5 | 19.5 | 17.5 | 17.5 | 19.5 | 21.5 | 21.5 | 23.5 |
| Los Angeles | | 17.5N | 19.5 | 19.5 | 20.6 | 20.5 | 21.5 | 19.5 | 17.5 | 17.5 | 19.5 | 19.5 | 22.5 |
| | NEC | | | | | | | | | | | | |
| | | 8.5 | 7.5 | 7.5 | 7.5 | 8.5 | 8.5 | 8.5 | 9.5 | 10.5 | 10.5 | 10.5 | 9.5 |
| | NECC | | | | | | | | | | | | |
| | | 3.5N | 4.5 | 2.5 | 2.5 | 2.5 | 4.5 | 2.5 | 4.5 | 4.5 | 3.5 | 3.5 | 3.5 |
| | | 2.5S | 2.5 | 2.5 | 2.5 | 2.5 | 2.5 | 2.5 | 2.5 | 2.5 | 2.5 | 2.5 | 2.5 |
| | SEC | | | | | | | | | | | | |
| Tahiti | | 15.5S | 15.5 | 17.5 | 17.5 | 17.5 | 19.5 | 19.5 | 19.5 | 19.5 | 19.5 | 19.5 | 19.5 |
| Panama | | 2.5S | 2.5 | 2.5 | 2.5 | 2.5 | 2.5 | 2.5 | 2.5 | 2.5 | 2.5 | 2.5 | 3.5 |
| | SEC | | | | | | | | | | | | |
| Mururoa | | 17.5S | 18.5 | 18.5 | 16.5 | 17.5 | 21.5 | 17.5 | 17.5 | 16.5 | 16.5 | 16.5 | 16.5 |

calculated from bimonthly averaged temperature sections, rather than synoptic sections. In a two-layer model with the bottom layer at rest, the transport ($T$) of a current is:

$$T = -\frac{g'}{f} \Delta D \cdot \bar{D} = -\frac{g'}{2f}\left(D_N^2 - D_S^2\right) \qquad (1)$$

where $D_N$ and $D_S$ are the depth of the interface on the northern and southern edges of the current, $g'$ is the reduced acceleration due to gravity, $f$ is the Coriolis parameter, $\Delta D$ is the depth difference across the current and $\bar{D}$ is the mean depth of the current. The standard error ($E$) of the bimonthly mean transport estimated from mean values of depth is according

*Table 4. Long-term annual mean transport in Sverdrups ($10^6$ m$^3$/s) of the North Equatorial Current, North Equatorial Countercurrent and South Equatorial Current. The longitude where the XBT track crosses the current is given*

| | Port Hedland–Japan | Noumea–Japan | Auckland–Hawaii | Tahiti–Los Angeles | Mururoa–Panama |
|---|---|---|---|---|---|
| | 30.1 | 24.2 | 15.3 | 8.0 | |
| NEC | 130°E | 150°E | 154°W | 130°W | |
| | 26.8 | 21.0 | 14.2 | 12.0 | |
| NECC | 127°E | 153°E | 156°W | 136°W | |
| | | 16.5 | 30.2 | 33.1 | 23.0 |
| SEC | | 160°E | 160°W | 145°W | 110°–150°W |

to Ku (1966):

$$E = \frac{2C\sigma}{\sqrt{n}}\left[\langle D_N\rangle^2 + \langle D_S\rangle^2\right] \tag{2}$$

where $C$ is $g'/2f$, $\langle D_N\rangle$ and $\langle D_S\rangle$ are the long-term mean values, $\sigma$ is the standard deviation of $D_N$ and $D_S$, and $n$ is the total number of transects across the current during a bimonth. Note that (2) is similar to the estimate of standard deviation but smaller by the factor $1/\sqrt{n}$. The derivation of this formula assumes that variations of $D_N$ and $D_S$ are not correlated, that they are small compared to long-term mean values, and that $\sigma$ is equal on either side of the current. The assumptions require justification. Variations of the depth of the 20°C isotherm throughout the tropical Pacific have been carefully documented by Meyers *et al.* (1989). The standard deviation summarised in their Table 4 shows some variation with location, but the differences are not large enough to alter the estimates of standard error given below. The standard deviation of isotherm depth in their study has a median value of 23 m, which is used as the value for $\sigma$ in (2). $\sigma$ is much smaller than mean values of $D_N$ and $D_S$, except on the northern side of the NECC, where $\sigma$ is smaller by only a factor of 2–4. The correlation between $D_N$ and $D_S$ for the NECC was shown to be small (0.26) for a 20 year period by Wyrtki (1978). The small correlation over a long period of time occurs because $D_N$ and $D_S$ in the NECC are positively correlated when El Niño or La Nina conditions are dominant, while they are negatively correlated when the seasonal oscillation is dominant (Meyers *et al.*, 1989, Figs 11B and 13B). The correlation between $D_N$ and $D_S$ for the SEC and the NEC is small (Meyers *et al.*, 1989, Figs 11E and 13E) because the currents are wide (> 1000 km) while small, energetic eddies of about 100 km width strongly affect the depth at boundaries of the currents. Small positive correlations between $D_N$ and $D_S$ would slightly increase estimates of the standard error of bimonthly mean transport calculated from (2). However, it is important to note that the standard errors discussed below depend above all on the factor $1/\sqrt{n}$, that is the number of sections available for the study. The results on standard error of the mean are not strongly influenced by the slight differences between the assumptions made above and the real ocean.

The results of estimating standard errors with (2) are summarised in Table 2, which also shows the total number of XBT drops on each line, and the total number of transects obtained during the study period. The number of transects obtained during a bimonth was estimated as the total divided by 6. The values of $D_N$ and $D_S$ were measured from the long-term annual mean temperature sections in Fig. 2. The value of $g'/2f$ (called $C$ in the table) was estimated for each current and each transect by the value that makes the right hand side

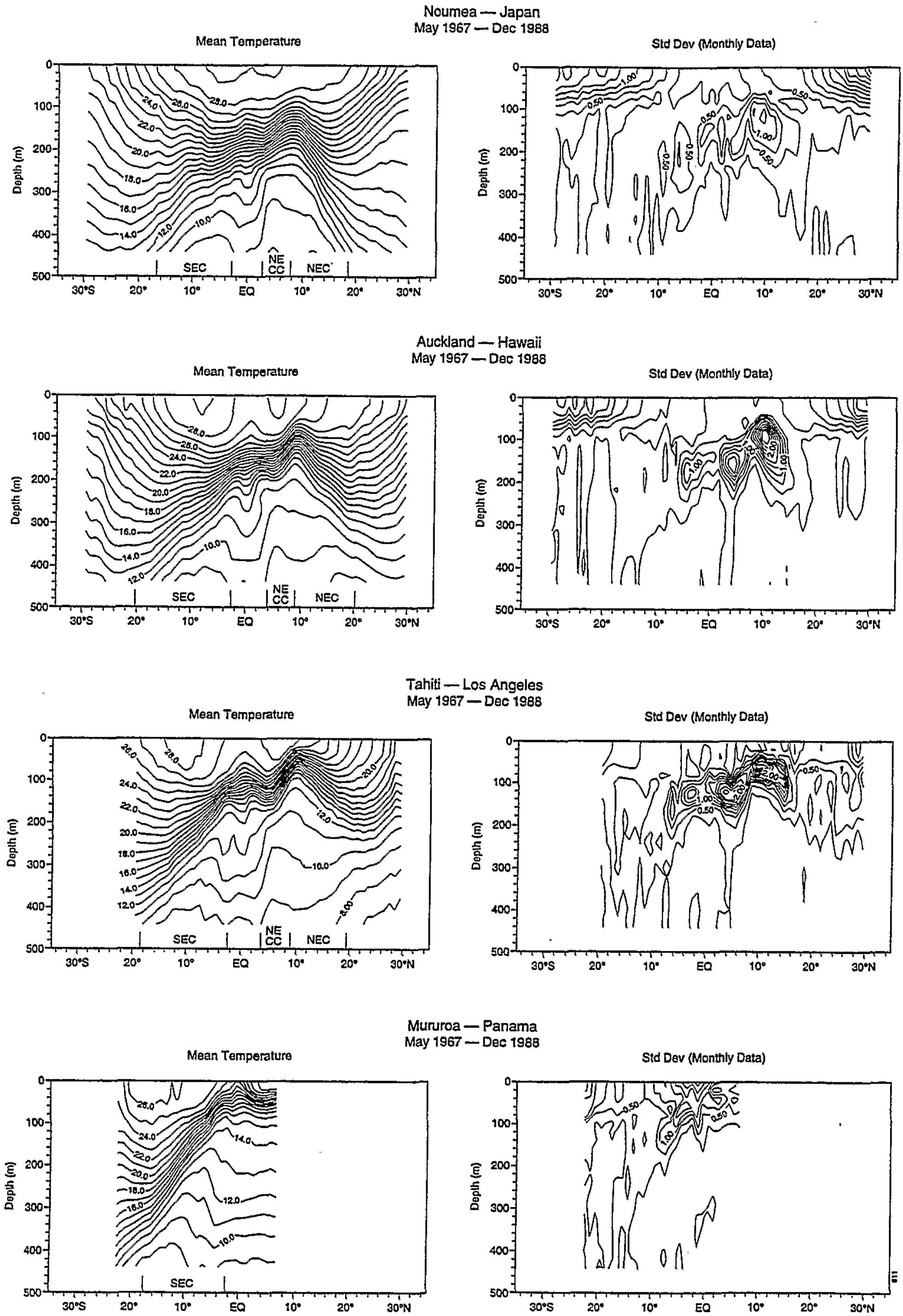


Fig. 2. Long-term annual mean temperature sections (left) and standard deviation of bimonthly mean temperatures (right) in °C.

of (1) equal to the observed long-term annual mean transport, which is discussed later. $C$ estimated in this way depends as much on the density-stratification as it does on the Coriolis parameter. The standard deviation of transport estimated from (2) with $n = 1$ is in the range 5–15 Sv. Generally, it increases from east to west, following the deepening of the thermocline toward the west. The standard error of bimonthly mean transport ($E$) is in the range 0.8–5.6 Sv and depends strongly on $n$. The most accurate estimates of long-term bimonthly mean transport are on the oldest line, Auckland to Hawaii. The standard errors are in the range 1–2 Sv for most of the currents and lines.

Statistical errors due to variations in the $T/S$ relationship generally have a small effect on the calculation of dynamic height and geostrophic transports. For example, RMS errors in dynamic height due to use of a mean $T/S$ relationship are often in the range of 2–4 dynamic cm (Taft and Kessler), which is much smaller than the variations due to eddies discussed above. However, while errors due to eddies will tend to average out with more data, errors due to a faulty mean $T/S$ curve might introduce a bias in our transport calculations.

## THERMAL STRUCTURE

The long-term annual mean and standard deviation of the bimonthly mean temperatures on four of the sections are presented in Fig. 2. The westernmost section (not presented) is the newest one and is based on relatively few data. The thermal structure is an essential aspect of the Equatorial Current System (Wyrtki and Kilonsky, 1984), closely related to the vertical and meridional gradients of the flow-field. It is described here because it is the best observed feature of the currents. The standard deviation may be useful for validation of ocean general circulation models of annual variation.

The sections show the ridges and troughs of the thermocline already defined in earlier studies (Wyrtki, 1978; Donguy and Henin, 1983; Wyrtki and Kilonsky, 1984). The most prominent feature is the NECC ridge (in the thermocline) near 10°N on the Noumea–Japan, Auckland–Hawaii and Tahiti–Los Angeles tracks. The equator shows upwelling at the surface and spreading of the thermocline associated with the Equatorial Undercurrent on all the sections. Between the equator and 10°N a trough separates the SEC from the NECC. It is worth noting that the NECC is rather a shallow current, and that a deep temperature gradient under its southern side is directly related to a Deep Countercurrent (DC), which is a dynamically independent component of the general circulation (McPhaden, 1984). In estimating transport of the NECC as the total flow between the ridge and trough of the 0/400 db vertically integrated dynamic height, part of the transport of the DC is included in the NECC. This point is raised again in comparing our results to earlier studies. Away from the equator, the NEC and the SEC (south of 2.5°S), which could be termed SEC (S), are characterised by a downward slope of the thermocline toward the poles. Between 5°S and 10°S, particularly in the western Pacific, isotherm shallowing toward the pole is consistent with the existence of SECC. The thermocline gets deeper from east to west. Associated with the deepening is a decrease of the vertical temperature gradient. The meridional slope of isotherms also decreases from east to west.

The standard deviation of bimonthly mean temperature has a maximum between 12°N and 10°S in the thermocline. The largest values are found on the lines in the central Pacific, where the standard deviation exceeds 2°C in the NECC ridge. Relative maxima appear on both sides of the equator, due to change in the vertical gradient.

## LONG-TERM MEAN TRANSPORTS

The major currents described here are the westward NEC from about 20°N to 8°N, the eastward NECC from 8°N to 4°N and the westward SEC (S) south of 2.5°S. The boundaries of these currents for each bimonth are presented in Table 3.

The long-term annual mean 0/400 db transports were calculated from the bimonthly transports. The mean boundaries are indicated on Fig. 2. The transport of the NEC increases regularly toward the west (Table 4) from 8.0 Sv at 134°W on the easternmost track to 30.1 Sv at 130°E on the westernmost. The NECC transport also increases regularly toward the west (Table 4) from 12.0 Sv on the easternmost track at 136°W–26.8 Sv on the westernmost at 127°E. The increasing transports of the NEC and the NECC toward the west as noted by Kendall (1970) develop because the flow occurs mostly above the thermocline and is associated with increasing depth of the thermocline from the east to the west, which is qualitatively consistent with the two-layer model of transports in (1). The increase is also qualitatively consistent with Sverdrup transports calculated from wind stress curl (Meyers, 1980).

The SEC (S) is considered only in the southern hemisphere south of 2.5°S, neglecting its parts on the equator and in the northern hemisphere. Its transport is 23.0 Sv on the Mururoa–Panama track, 33.1 Sv on the Tahiti–Los Angeles, 30.2 Sv on the Auckland–Hawaii and 16.5 Sv on the Noumea–Japan. The decrease in transport west of Tahiti is due to substantial flow below 400 m as the current gets increasingly deep toward the west. Eastward currents within the SEC (S) were weak in the bimonthly averages for the eastern and central Pacific. On the Noumea–Japan track the SECC was located at 10°S with a transport of 1.5 Sv and the South Tropical Countercurrent was located at 15°S with a transport of 2.2 Sv. The eastward flows were not added into the estimates for the SEC (S). It is difficult to point out clear annual variations of such weak eastward flow: the bimonthly average may be unable to capture them and in the south western Pacific, eastward transports are more dependent on ENSO than on the season (Donguy *et al.*, 1984).

## MEAN ANNUAL VARIATION

The bimonthly transports for the NEC, NECC and SEC (S) are displayed in Figs 3–5 in radial coordinates, where the distance from the origin represents transport and the angle represents time during an annual cycle. The annual variation of the NEC (Fig. 3) is small, as noted in earlier studies. It is worth recalling here that Taft and Kessler (1991) noted a strong annual cycle of the sea-level difference between Honolulu and Kwajalein which is representative of changes in the latitude of the current but not its total transport. The annual range in the eastern Pacific (Tahiti–Los Angeles track) is between 8 and 10 Sv (22% of the mean value). Larger variations relative to the mean occur in the western Pacific (Port Hedland–Japan track), probably due to the strong forcing by monsoon winds with a minimum transport in July/August (27 Sv) and a maximum in January/February (36 Sv) (29% of the mean value). The largest variations relative to the mean are in the central Pacific (Auckland–Hawaii track) with a maximum in November/December (18 Sv) and minimum in March/April (13 Sv) (32% of the mean value). Averaged over the basin the tendency is to have a maximum transport between December and February. While the amplitude of the annual variation of the NEC transport presented in this study is small, it is somewhat larger than in other studies. For example, Taft and Kessler (1991) found an annual amplitude of 1.6 Sv (9% of the mean value).

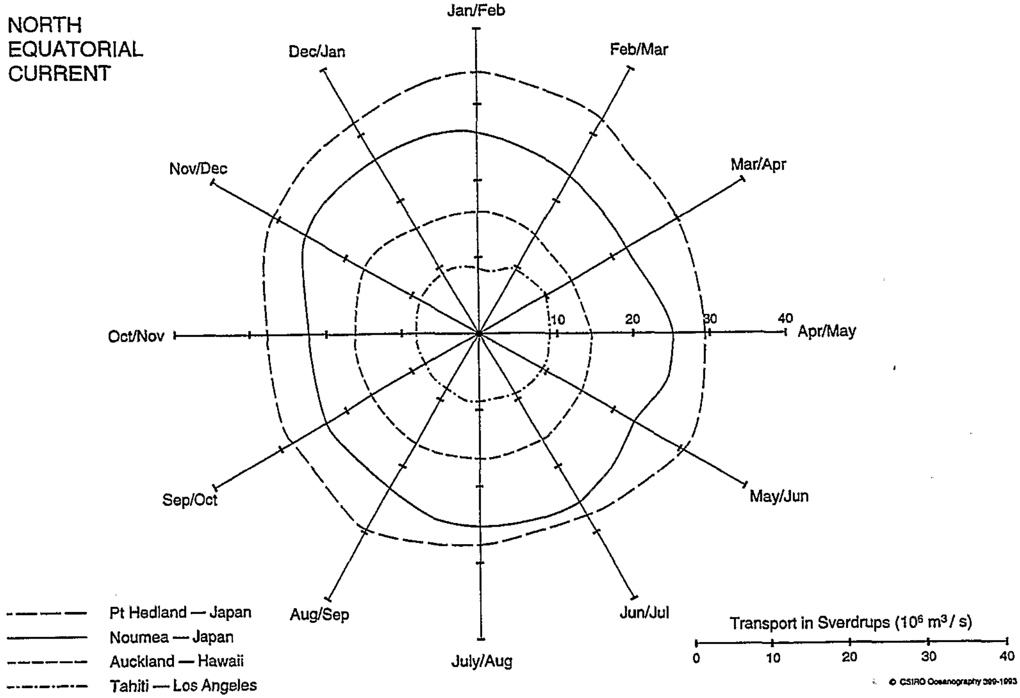


Fig. 3. Annual cycle of the geostrophic transport of the North Equatorial Current calculated from bimonthly mean temperatures using a mean temperature/salinity relationship. The transports in Sverdrups are indicated by distance from the origin.

The NECC has a prominent annual cycle (Fig. 4) on all four tracks. The minimum appears during March to June: May/June (5 Sv) on Tahiti–Los Angeles; April/May (5 Sv) on Auckland–Hawaii; March/April (11 Sv) on Noumea–Japan; and June/July (14 Sv) on Pt Hedland–Japan. A secondary minimum is apparent in September/October. The maximum appears during December to February: December/January (19 Sv) on Tahiti–Los Angeles; December/January (25 Sv) on Auckland–Hawaii; November/December (29 Sv) on Noumea–Japan; and February/March (43 Sv) on Pt Hedland–Japan. A secondary maximum appears during June–August, strongest in the west. The NECC transport is maximum in December due to variation of the wind stress curl associated with the Intertropical Convergence Zone (Sadler *et al.*, 1987; Kessler, 1990).

The annual cycle of the SEC (S) shows a change in phase from line to line (Fig. 5). The Tahiti–Los Angeles and Noumea–Japan tracks have maximum transport during January–May while the Auckland–Hawaii and Mururoa–Panama tracks have a maximum during July–October. The phase changes do not have an obvious explanation.

The SEC (S) has two distinct branches on the track between Noumea and Japan, separated by the SECC at 10°S. The variation of the two branches is shown in Fig. 6. The westward transport between 2.5°S and 10°S has an annual cycle different to the one between 10°S and 20°S. The first one is maximum from January to June; the second one from July to December. This result is not consistent with the prevalence of west wind from January to June between 2.5°S and 10°S (Wyrtki and Meyers, 1975). However, this might be the result

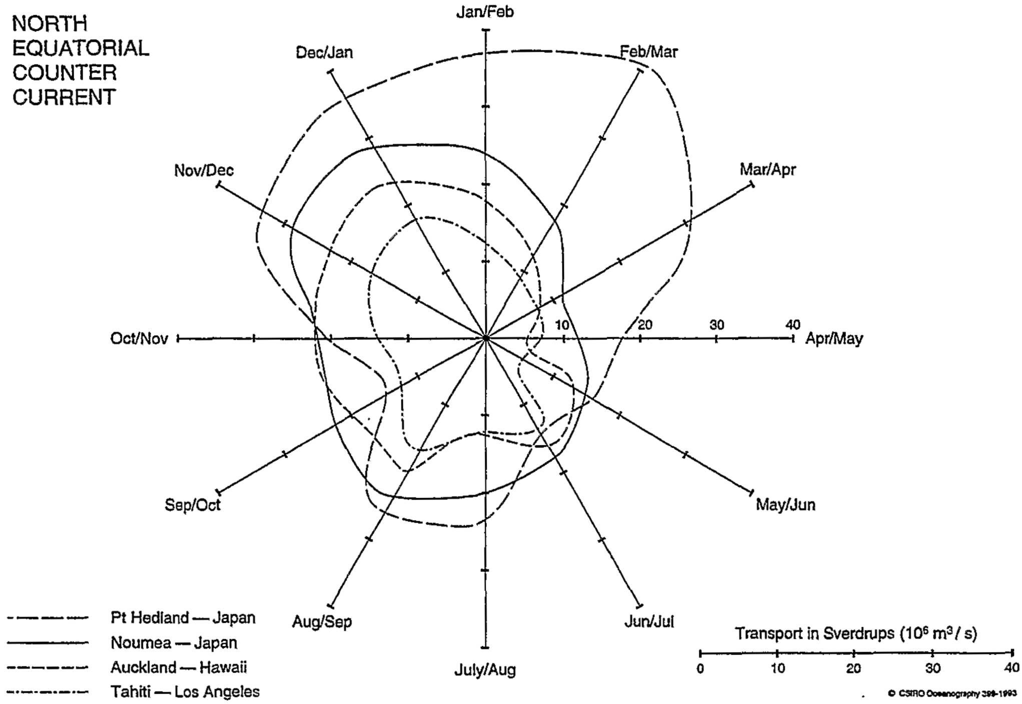


Fig. 4. As Fig. 3 except for the North Equatorial Countercurrent.

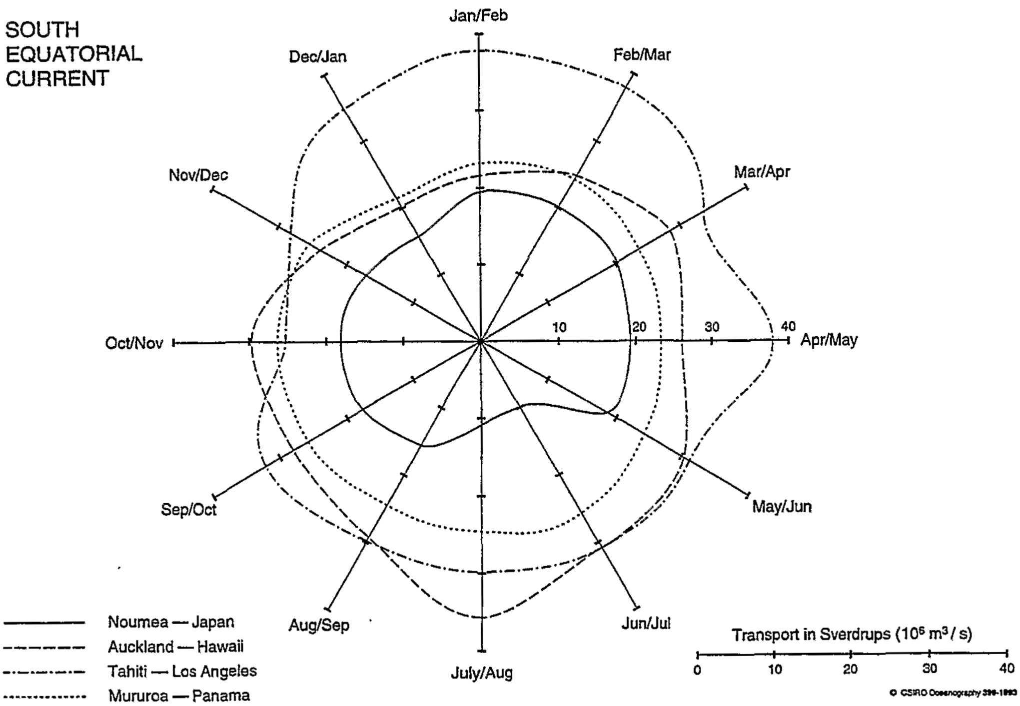


Fig. 5. As Fig. 3 except for South Equatorial Current.

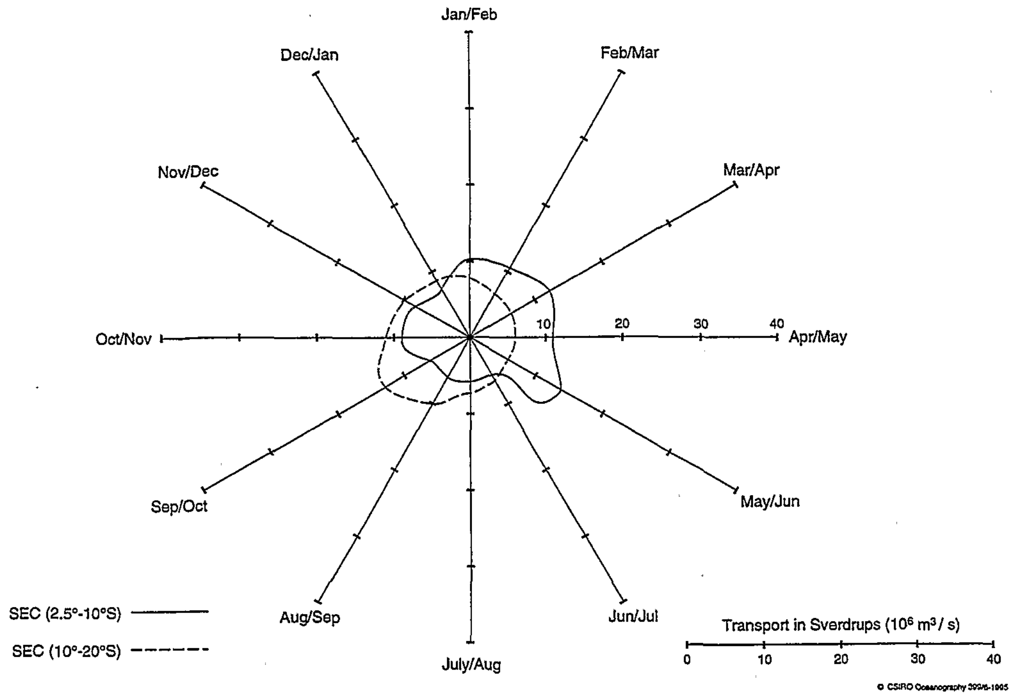


Fig. 6. As Fig. 3 except for the two components of the South Equatorial Current (2.5°S–10°S, full line; 10°S–20°S, dashed line) along the Noumea–Japan track.

of the southward shift of the positive curl due to the presence of the South Pacific Convergence Zone (Kessler and Taft, 1987) in this area during southern summer.

## COMPARISON TO EARLIER STUDIES

The earlier studies by Kessler and Taft (1987), Taft and Kessler (1991) and Picaut and Tournier (1991) describe the transport of the major tropical currents in the Pacific, with an emphasis on interannual variation and the central Pacific. Although mean annual variation was not the specific target of these studies, their results from the central Pacific can be directly compared to ours (Table 5). Several differences in numerical values are larger than the stochastic errors given in Table 2 and require discussion. They are caused by differences in the analysis procedures used in the studies, as discussed in detail below. One of the surprising results of this study was learning that the procedures can have such a large impact. This should be borne in mind in any attempt to use the results of any of the studies for applications such as model-comparison studies. The differences in procedure are described below under four categories.

1. The period of data-coverage is not the same. Kessler and Taft used 1979–1984. Taft and Kessler extended the coverage to 1970–1987. Picaut and Tournier used data from 1979 to 1985. The present study (called DM below) takes into consideration data from the period 1967–1988. Moreover, only Taft and Kessler estimated the mean annual cycle of transports, and for this they used data for the period 1974–1981 to avoid including data from the 1972–

*Table 5. Comparison of results for the central Pacific from four studies (see text for details)*

| Study | Period | Area | Data | NEC mean phase | NECC | SEC mean phase | Theme | Important results |
|---|---|---|---|---|---|---|---|---|
| KT | 79–84 | Fiji to Hawaii | XBT | 17.0 Sv (450 db) | 21.1 Sv (450 db) | 35.1 Sv (450 db) | Interannual variability | Ekman pumping |
| TK | 70–87 | Pago Pago to Hawaii | XBT sea level | 18.1 Sv Nov/Dec | 15.6 Sv Sept/Oct | 36.2 Sv April/May | Annual and interannual variability | 1972/3 1982/3 ENSO |
| PT | 78–85 | Fiji–Hawaii Noumea Japan | XBT CTD Hydrocast | 15.7 Sv | 17.8 Sv | 33.2 Sv | Interannual variability Equatorial currents | Equatorial transports and currents |
| DM | 67–88 | Five lines all Pacific | XBT | 15.3 Sv Nov–Dev | 14.2 Sv Nov/Dec | 30.2 Sv Jul/Aug | Mean annual cycle | Whole Tropical Pacific |

73 and 1982–83 ENSOs, which impact strongly on the NECC and SEC (Meyers, 1982; Meyers and Donguy, 1984; Donguy *et al.*, 1984). The annual phase of NEC transport given by Taft and Kessler and DM is in good agreement, but differences as large as three months are found for the NECC and SEC, which may be due to the period of data coverage. This study used all of the available XBT data so that the results will be comparable to models of the ocean general circulation driven by climatological winds.

2. The areas selected to represent meridional sections are different. DM used all the tracks that have proven to be the most frequently repeated since 1972 and selected data in a band of width 12 centered on a line between the end-ports. The areas are considerably smaller in width than those used by Taft and Kessler and Picaut and Tournier who wanted to maximise the number of captured data to study interannual variation. The central Pacific band was centered on Auckland–Hawaii by DM, on Pago Pago–Hawaii by Taft and Kessler and on Fiji–Los Angeles by Picaut and Tournier. DM covered a wider band of latitude (30N–30S) than the other studies, which were limited to 20 or 25N or S. The different areas may be the cause of differences in the results, particularly at the poleward ends of the sections affecting the NEC and SEC.

3. The basic data used in all the studies are from the XBT project operating out of Noumea since 1979 (Meyers and Donguy, 1980), supplemented by the XBT file from NODC. Taft and Kessler and Picaut and Tournier supplemented their analyses with sea level or hydrographic data and sea level difference to measure geostrophic flow. Picaut and Tournier obtained a large number of additional XBTs from the French Navy. The slightly different data sources are not likely to be the source of differences in the results.

4. The definition of boundaries of the currents and the processing of data near the ends of the sections was quite different in the four studies, due to differences in the primary goal of each study. Kessler and Taft, Taft and Kessler and Picaut and Tournier were primarily interested in interannual variations and consequently identified the boundaries of currents on monthly velocity sections as a function of depth. Due to the presence of eddies and internal waves, selecting the northern and southern edges of a current is sometimes difficult on a synoptic monthly section and subjective choices have to be made. The tendency is to choose the boundaries at the absolute maximum and minimum of dynamic height. DM estimated the boundaries from long-term, bimonthly averaged fields, which largely eliminated the effect of eddies. We believe the difference in selecting boundaries is in part the cause of generally smaller values of transport estimated by DM (Table 5), in particular

for the NECC. However, as Kessler and Taft does not include the deep Countercurrent in the NECC transport, the difference with DM is particularly important.

Taft and Kessler and Picaut and Tournier defined the boundaries of the NEC and SEC as all the westward flow in the meridional section within 8–25N or 2–20S. This definition also biases the monthly transport toward larger values by neglecting the cancellation of eastward and westward flow in eddies within the central part of the current (Wyrtki, 1982). The poleward boundary of the currents often slopes to higher latitude with depth, which was carefully considered by Taft and Kessler. Taft and Kessler also made a careful inspection of the velocity section to find the sloping boundary between the NECC and deep Countercurrent. DM in contrast selected the boundaries from ridges and troughs in the vertically integrated dynamic height, and calculated the transport as an integral over all the flow between the boundaries. There was no ambiguity to the definition in the long-term bimonthly averaged fields. DM also had the northern boundary of the SEC at 2.5S. The different procedures may again be the cause of generally smaller values estimated for the NEC and SEC by DM (Table 5).

Picaut and Tournier were also primarily interested in calculating currents at the equator. Very careful smoothing of the dynamic height field by an adaptation of harmonic analysis was required for this calculation. While this procedure works well near the equator in the central part of a section, it introduces artificial data at the high latitude ends of the section. This procedure may account for the smaller values of NEC and SEC transports estimated by Picaut and Tournier in comparison to Taft and Kessler (Table 5).

## COMPARISON TO MODEL STUDIES

The long-term mean and annual variation of transports of major currents in a model of the Pacific Ocean has been described in the study by Philander *et al.* (1987). This is to our knowledge the only published model-study that presents the transports in a format that can be compared to the observational studies. The model-ocean was divided into boxes representing five bands of longitude approximately representative of areas covered by the XBT tracks. The boxes representing 2.5–10N can be compared to observations of the NECC and the boxes representing 2.5–10S can be compared to our results for the SEC. The mass transport was presented for the upper 50 m, 50–317 m and below 317 m. The total transport of the model is compared to the observations.

For the NECC the model consistently has a smaller long-term mean transport than our observations. In the vicinity of the Noumea–Japan track the model has a transport of 12.3 Sv compared to the observed 21.0 Sv. In the vicinity of the Auckland–Hawaii track it has 6.8 Sv compared to 14.2 Sv. In the vicinity of the Tahiti–Los Angeles track it has 6.6 Sv compared to 12.0 Sv. The annual cycle of transport in the model presented for 154°W and 180°W shows a phase similar to our observations, with the minimum occurring in March-April–May at both longitudes and the maximum in November near the dateline and one to two months earlier in the central Pacific.

The comparison for the SEC is limited because the model-results are presented to 10°S whereas our results are representative of the whole current to about 20°S. The model gives 20.5 Sv instead of 16.5 near the Noumea–Japan track, 22.4 Sv instead of 30.2 Sv near the Auckland–Hawaii track and 4.9 Sv instead of 23.0 Sv near the Mururoa–Panama track. Near 150°W the model gives maximum transport from January to May in agreement with our observations on the Noumea Japan track. Near 110°W the model gives maximum transport from July to October in agreement with our observations on the Mururoa–Panama track.

The most important difference between the model and our observations is the models relatively weak eastward transport of the NECC, which may be, at least in part, due to the choice of fixed boundaries for the current in the model, as opposed to choosing the ridge and trough in the observations. The weak simulation of NECC could also be due to the use of monthly average climatological winds, which may have smoothed the field of wind stress curl.

The seasonal cycle of transports of major Pacific currents in the Semtner and Chervin (1992) model was documented by Gordon (1992). The transports of NEC, NECC and SEC were evaluated in the upper 310 m. In contrast to the model by Philander *et al.* (1987), Gordon (1992) presents transports that are considerably larger than the observed 0/400 db transports. The model transports are larger by a factor typically of 1.5 in the NECC and 2 in the NEC. The SEC in the model cannot be compared to our results because its transport was not evaluated in the same latitude band as ours. Possible sources of the discrepancy are the Ekman currents in the model and the reference level in our geostrophic calculations.

The annual variation of the NEC in the model is small relative to the mean as in the observations. The model phase is nearly six months out of phase with the observations. We cannot suggest an explanation for the difference.

The annual variation of the NECC is relatively larger. The phase of the annual cycle of the model-NECC is on average across the basin similar to the observed phase, but precedes it by about two months. The important discrepancy is that the date of maximum and minimum transport propagates westward in the model but appears in the same season on all the tracks in the observations. The phase of the model matches the observations best for the Auckland–Hawaii track, including the minimum in April/May and the broad maximum from October through December. The westward progression suggests that wave dynamics plays a greater role in the model than in the observed, averaged annual cycle. This apparent discrepancy might be an artefact of forcing the model with a perfectly repeating cycle of the wind field, and intermittently sampling the real ocean with its strong interannual variability.

## CONCLUSION

All the available XBT profiles on five frequently repeated tracks were used with the climatological *T/S* relationship to document mean annual variation of the volume transport relative to 400 db of major currents throughout the tropical Pacific Ocean. Variation of the NEC is small. The long-term mean increases regularly toward the west from 8.0 Sv at 130°W to 30.1 Sv at 130°E. Variation of the NECC has a maximum between November and February, which occurs progressively later toward the West. The SEC has a distinctive annual variation, with phase differences from track to track. The stochastic errors in the estimates of bimonthly mean transport are relatively small, 1–2 Sv, due to the large number of repeat sections on most of the tracks. The results of this study differ from the results of earlier studies by more than 2 Sv in many cases, and the cause of the differences is traced to differences in details of the data processing, in particular to how boundaries of the currents are defined and to the period of data coverage. In future comparisons of observed transports of the major currents to the results of ocean general circulation models it would be debatable if this study or the earlier studies might be preferable to use. An advantage of this study is that the procedure is easy to duplicate and almost completely objective, making it easy to update as the number of transects increases in the future. It also covers all of the tropical Pacific in contrast to the earlier studies.

Studies taking into account variability of major currents throughout the tropical Pacific are rare. Due to the XBT network, it has been possible to assemble an overview of the annual cycle of the major currents and associated thermal structure. The description provides a robust data set for use in validation of ocean general circulation models.

*Acknowledgements*—Volunteer observers on merchant ships have generously collected the XBT data. T. Qu calculated the mean temperature sections and transport functions. W. Kessler allowed us to use his XBT data after very careful quality control. He and an anonymous referee made several valuable comments on a draft of the paper. We gratefully acknowledge this support.

## REFERENCES

Cantos-Figuerola A. and B. A. Taft (1983) The South Equatorial Current during the 1979–80 Hawaii–Tahiti Shuttle. *Tropical Ocean–Atmosphere Newsletter*, **19**, 6–8.

Delcroix T., G. Eldin and C. Henin (1987) Upper ocean water masses and transport in the western tropical Pacific (165°E). *Journal of Physical Oceanography*, **17**, 2248–2262.

Donguy J. R. and C. Henin (1983) Fluctuations of the equatorial current system connected with the hydroclimatic conditions in the western Pacific. *Oceanogr. Trop.*, **18**, 17–24.

Donguy J. R., G. Eldin, A. Morliere and J. P. Rebert (1984) Variability of dynamic topography and equatorial currents in relation to hydroclimatic conditions of the Western Pacific. *Oceanogr. Trop.*, **19**, 155–160.

Donguy J. R., G. Eldin and K. Wyrtki (1986) Sea level and dynamic topography in the western Pacific during 1982–1983 El Niño. *Tropical Ocean–Atmosphere Newsletter*, **36**, 1–3.

Eldin G. (1983) Eastward flows of the south equatorial central Pacific. *Journal of Physical Oceanography*, **13**, 1467–1481.

Gordon L. J. (1992) *Analysis of a simulation of the seasonal cycle in the tropical Pacific Ocean in an eddy-resolving global ocean model.* Thesis Master of Science in Meteorology and Oceanography, Naval Postgraduate School, Monterey, CA, 75 pp.

Hayes S. P., J. M. Toole and L. J. Mangum (1983) Water mass and transport variability at 110°W in the equatorial Pacific. *Journal of Physical Oceanography*, **13**, 153–168.

Harrison D. E., W. S. Kessler and B. S. Giese (1989) Ocean Circulation Model hindcasts of the 1982–1983 El Niño: thermal variability along the ship-of-opportunity tracks. *Journal of Physical Oceanography*, **19**, 397–418.

Kendall T. R. (1970) The Pacific Equatorial Countercurrent. International Centre for Environmental Research, 19 pp.

Kessler W. S. (1990) Observations of long Rossby waves in the northern tropical Pacific. *Journal of Geophysical Research*, **95**, 5183–5217.

Kessler W. S. and B. A. Taft (1987) Dynamic heights and zonal geostrophic transports in the central Pacific during 1979–84. *Journal of Physical Oceanography*, **17**, 97–122.

Ku H. H. (1966) Notes on the use of propagation of error formulae. *Journal of Research of the National Bureau of Standards—C. Engineering and Instrumentation*, **70C**, 331–341.

Levitus S. (1982) *Climatological atlas of the world ocean.* NOAA, Professional Paper No. 13, U.S. Department of Commerce, 173 pp.

McPhaden M. J. (1984) On the dynamics of equatorial subsurface countercurrents. *Journal of Physical Oceanography*, **14**, 1215–1225.

McPhaden M., A. J. Busalacchi and J. Picaut (1988) Observations and wind-forced model simulations of the mean seasonal cycle in tropical Pacific sea surface topography. *Journal of Geophysical Research*, **93**(C7), 8131–8146.

Merle J., H. Rotschi and B. Voituriez (1969) Zonal circulation in the tropical western South Pacific. In: *Perspectives in fisheries oceanography*. Japanese Society of Oceanography, Special Number 91–98.

Meyers G. (1980) Do Sverdrup transports account for the Pacific North Equatorial Countercurrent? Journal of Geophysical Research, **85**, 1073–1075.

Meyers G. (1982) Interannual variation in sea level near Truk Island—A bimodal seasonal cycle. *Journal of Physical Oceanography*, **12**, 1161–1168.

Meyers G. and J. R. Donguy (1980) Survey of XBT measurements from ships-of-opportunity in the tropical Pacific. *Tropical Ocean–Atmosphere Newsletter*, **2**, 6–7.

Meyers G. and J. R. Donguy (1984) The North Equatorial Countercurrent and heat storage in the western Pacific Ocean during 1982–83. *Nature*, **5991**, 258–260.

Meyers G., J. Sprintall, H. Phillips, J. Peterson and T. Fonseca (1989) Design of an ocean temperature observing network in the seas north of Australia. Part 1. Tropical Pacific Ocean—Statistics, CSIRO Marine Laboratories Report 204, Hobart, 50 pp.

Meyers G., H. Phillips, N. Smith and J. Sprintall (1991) Space and time scales for optimal interpolation of temperature—tropical Pacific Ocean. *Progress in Oceanography*, **28**, 189–218.

Philander S. G. H., W. J. Hurlin and A. D. Seigel (1987) Simulation of the seasonal cycle of the tropical Pacific Ocean. *Journal of Physical Oceanography*, **17**, 1986–2002.

Picaut J. and R. Tournier (1991) Monitoring the 1979–1985 equatorial Pacific current transports with Expendable Bathythermography Data. *Journal of Geophysical Research*, **96**(Suppl.), 3263–3277.

Sadler J. C., M. A. Lander, A. M. Hori and L. K. Oda (1987) Tropical Marine Climatic Atlas, Vol. 2. Pacific Ocean NOAA. Department of Meteorology, University of Hawaii, 3 pp.

Semtner A. J. and R. M. Chervin (1992) Ocean general Circulation from a global eddy-resolving model. *Journal of Geophysical Research*, **97**, 5493–5550.

Taft B. A. and W. S. Kessler (1991) Variations of zonal currents in the Central Tropical Pacific during 1970–1987: sea level and dynamic height measurements. *Journal of Geophysical Research*, **96**, 12,599–12,618.

Wyrtki K. (1974a) *The dynamic topography of the Pacific Ocean and its fluctuations*. Hawaii Institute of Geophysics HIG 74–5, 19 pp.

Wyrtki K. (1974) Sea level and the seasonal fluctuations of the equatorial currents in the Western Pacific Ocean. *Journal of Physical Oceanography*, **4**, 90–103.

Wyrtki K. (1978) Monitoring the strength of equatorial currents from XBT sections and sea level. *Journal of Geophysical Research*, **83**, 1935–1940.

Wyrtki K. (1982) Eddies in the Pacific North Equatorial Current. *Journal of Physical Oceanography*, **12**, 746–749.

Wyrtki K. and R. Kendall (1967) Transports of the Pacific Equatorial Countercurrent. *Journal of Geophysical Research*, **72**, 2073–2076.

Wyrtki K. and B. Kilonsky (1984) Mean water and current structure during the Hawaii to Tahiti Shuttle Experiment. *Journal of Physical Oceanography*, **14**, 242–254.

Wyrtki K. and G. Meyers (1975) *The trade windfield over the Pacific Ocean*. Hawaii Institute of Geophysics HIG 75–1, 25 pp.